

# **DETERMINATION OF CONTRAILS FROM SATELLITE DATA AND OBSERVATIONAL RESULTS**

U. Schumann and P. Wendling

DLR, Institute of Atmospheric Physics,  
D-8031 Oberpfaffenhofen, Germany

## **ABSTRACT**

Condensation trails (contrails) from air traffic in the upper troposphere may have an effect on the earth's climate. We first discuss the state of knowledge. Then some results of radiation transfer calculations are reported which help to estimate the order of magnitude of the effects of cirrus clouds and water vapour in comparison to doubling of the concentration of  $CO_2$ . The main part of the paper describes the analysis of contrails from satellite data. Based on NOAA-AVHRR data we present results for a specific case where contrails covered a few percent of a region including southern Germany and the Alps. Preliminary results are reported for 99 further cases. A pattern recognition method is described to identify contrails and the related cloud cover automatically. Laser observations reflect contrail cross-sections which are several km in width and about 700 m thick. The optical thickness reaches values up to 1.

## **INTRODUCTION**

It is known that thin cirrus clouds of large (more than about  $3\mu m$  in radius) ice particles in the upper troposphere at low and mid latitudes act to enhance the "greenhouse effect" owing to their rather high emissivity and low albedo (Stephens and Webster, 1981, Stephens, 1989). An increase in cirrus cloud coverage by a few percent might have the same effect as a doubling of the amount of  $CO_2$  (Liou, 1986). According to recent results of global circulation models (Wetherald and Manabe, 1988), clouds (for fixed radiation parameters; Stephens, 1989) tend to enforce the greenhouse effect induced by increasing  $CO_2$ .

Contrails from aircrafts enhance the appearance of high-level clouds. Such contrails emerge in particular at temperatures below  $-40^\circ C$  (Appleman, 1953). Such low temperatures prevail at the tropopause of the atmosphere where the radiation effect of absorbing material is strongest. The altitude of the tropopause varies from typically 8 km at high latitudes to about 18 km in the tropics. Thus, flight levels at mid-latitudes reach or exceed the tropopause. In view of the strongly increasing long-distance air traffic (an increase by a factor of two is expected by air traffic experts for the next decade) it is important to investigate the effects of contrail-induced cirrus clouds on climate more closely. The need for such investigations (in addition to studies of

changes in air chemistry by aircraft emissions) was stressed in several recent discussions (Held, 1988; Pfeiffer and Fischer, 1989).

Changnon (1981) reports about trends in cloudiness and sunshine based on routine surface observations for the time-period of 1901 to 1977 in the mid-west of the USA. He finds trends which seem to indicate an increase in cloudiness and decrease in sunshine duration in the period since 1960 and correlates this with the increasing fuel consumption by air traffic. Moreover, he finds a reduced temperature difference between day and night which might be caused by additional clouds. However, the data base for this analysis is too small to generalize such results. Angell (1990) reports on the cloud cover and sunshine duration at 100 stations within the whole USA. He compares mean values of the years 1950-68 with those in the years 1970-88 and shows that the cloud cover did increase by  $2.0 \pm 1.3$  from the first to the second period. The sunshine duration, however, decreases by only  $0.8 \pm 1.2\%$ . He explains this with the stronger increase of thin cirrus clouds which are observed as additional cloud cover but are still too thin to reduce the sunshine-duration measurements. Weber (1989) finds also a decrease in sunshine duration at several stations in Germany, but he argues that this originates from an increase in westerly flow bringing more clouds from the Atlantic over the continent. From a study of contrails recorded by a sky-camera over a period of one year in Kärnten/Austria, Rotter (1987) observed long-living contrails with a persistency of more than one hour and a cloud cover of up to 6 % on nine days. For the majority of the observations, the cloud cover was well below 1 %. Statistics on the frequency of contrails are also reported by Beckwith (1972). He found longliving contrails (more than 5 minutes persistency) in 25 % of all contrail observations from aircrafts at 13 km average flight level. Such observations are limited to a small region and confined to observations from the earth's surface or from aircrafts.

Satellite observations may provide objective measures to determine the cloud cover induced by contrails over a larger region. High resolution infrared satellite images often provide striking examples of contrails; corresponding visible images are usually less revealing (Joseph et al., 1975; Lee, 1989). Carleton and Lamb (1986) show that the occurrence of contrails can be determined from high-resolution (0.6 km in the visible and 1.0 km in the infrared spectral range) observations from the Defense Meteorological Satellite Program (DMSP). From a pilot study they find that contrails tend to occur frequently and often in association with natural cirrus clouds. Lee (1989) shows that data from the NOAA Advanced Very High Resolution Radiometer (AVHRR) can be used to produce images which greatly enhance contrails in comparison to the mono-spectral observations. He gives one example with little additional evidence on the meteorological conditions.

Except for in-situ measurements by Knollenberg (1972), little is known about the spatial structure and micro-physical parameters of contrails.

In this paper, we first discuss some estimates of the effects of water vapour and cirrus clouds near the tropopause on the heating rate of the atmosphere. Then results for a few cases are reported, mainly for the selected day of Oct. 18, 1989. For this day, ground observations, satellite data and Lidar observations will be presented. In particular, a new pattern recognition method will be described. The present study reports

work in progress. Much more effort is required before we can make final recommendations with respect to aspects of air traffic.

## RADIATION EFFECTS OF WATER VAPOUR AND CLOUDS

As stated before, thin cirrus clouds at higher levels have a strong effect on radiative heating. Fig. 1, taken from Liou (1986), shows results from a one-dimensional radiative transport model. The code is applied to compute infrared cooling (lower diagram) and solar heating (upper diagrams) rates for cloudy atmospheres using standard atmospheric temperature, water vapour and ozone profiles. Cirrus clouds with thicknesses of 0.1, 1, and 3 km are inserted in the atmosphere and a 100 % cloud cover is assumed. The base of the cloud is fixed at 8 km. For further parameters see Liou (1986). We see from the results that a cirrus cloud causes moderate heating by absorption in the solar range. The IR cooling rate reaches large values with a large cooling rate at the cloud top and a significant heating rate at the cloud base.

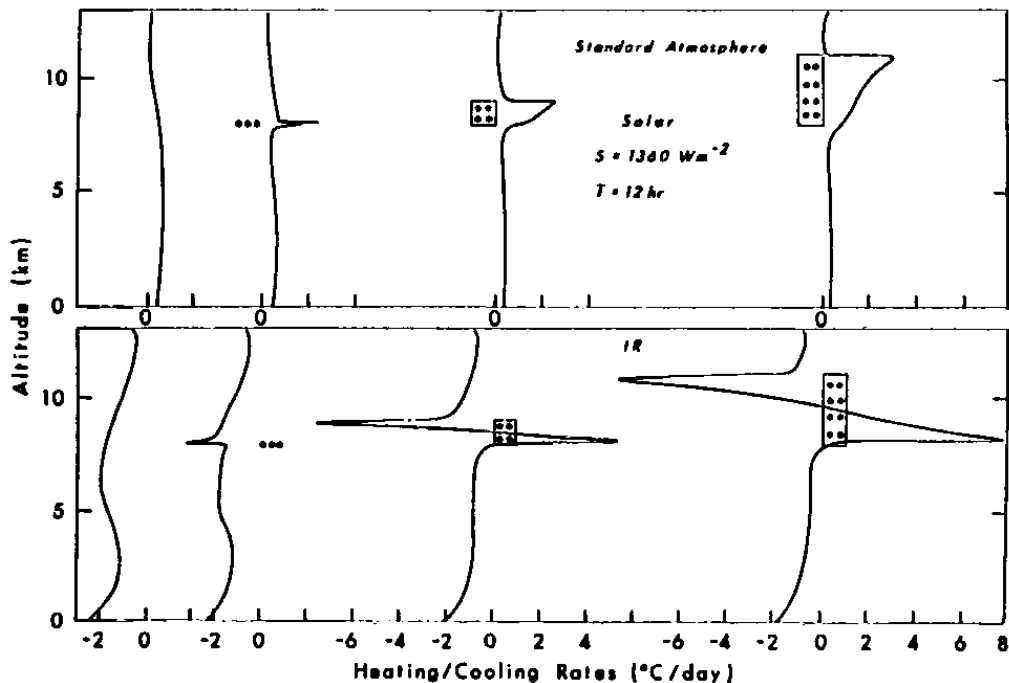


**Figure 1.** Thermal infrared and solar heating rates for cirrus clouds, taken from Liou (1986).

It should be noted that these are pure radiation calculations which do not reflect vertical transport processes induced in the atmosphere. Hence, the rather small effects of the clouds on the heating rate at the surface should not be misinterpreted. The vertical profile of cooling and heating will destabilize the layer taken by the cloud and thus induce additional vertical mixing, possibly with the effect of an increase in the altitude of the tropopause. Such an increase was found by Wetherald and Manabe (1988) and used to explain why high clouds in general tend to enhance the "greenhouse effect".

We have performed similar (but even simpler) radiation calculations with respect to the effects of increased water vapour. For the purpose of qualitative estimates, we investigate the change in infrared heating rate due to an increase of water vapour concentration (without clouds) in the altitude range from 9.5 to 14.5 km. We simply compare the results from two radiation calculations, one with the standard atmosphere and one with the water vapour increased up to local saturation with respect to water in the same atmosphere. The effect of changed water vapour concentration in the solar spectral range is negligible in comparison to that in the infrared. From Fig. 2 we see that the induced changes in heating rate due to changes in water vapour concentration (i.e. the difference between the dashed and the full curves) are qualitatively similar to the effects of cirrus clouds. However, the absolute magnitude is smaller. It is not small, however, in comparison to solar radiation effects of the cloud cases considered in Fig. 1.

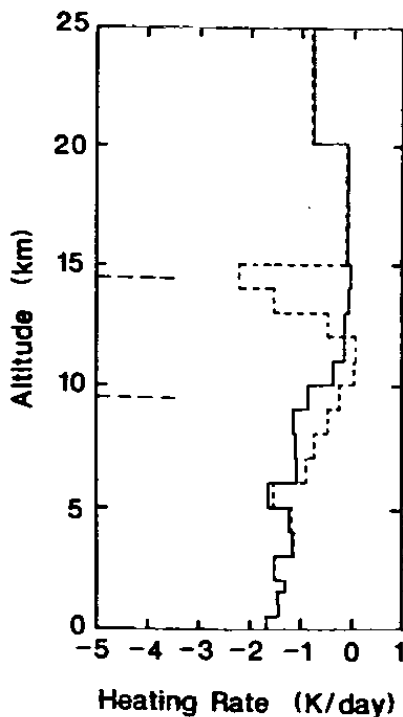


**Figure 2.** Thermal infrared heating rates for the standard atmosphere (full curve) and for the same case but with water vapour concentration increased up to saturation in the altitude interval from 9.5 to 14.5 km (dashed curve).

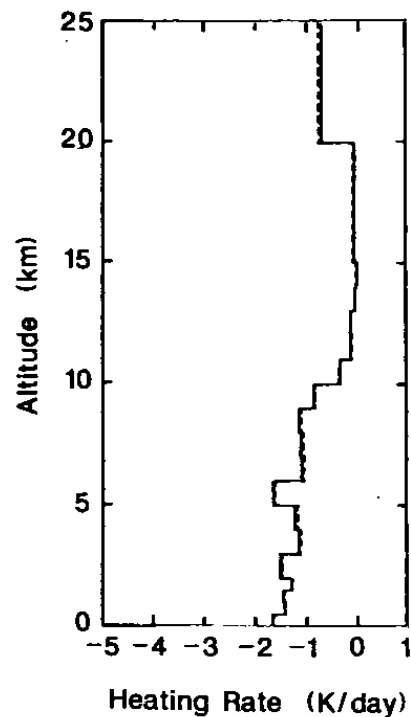


**Figure 3.** Thermal infrared heating rates for the standard atmosphere (full curve) and for the same case but with doubled  $CO_2$ -concentration at all levels.

For comparison, Fig. 3 depicts the infrared heating rate in the standard atmosphere for present and for doubled amount of  $CO_2$ , as computed in the same way. The change in heating rate due to doubled  $CO_2$  amounts to about 0.03 K/day at 8 km and -0.7 K/day at 25 km altitude. It is about two orders of magnitude smaller than that due to water vapour saturation in the 5 km interval near the tropopause. However, dou-

bling of  $CO_2$  influences the heating rate at all altitudes, especially in the upper stratosphere. Furthermore, one must note that the expected  $CO_2$ -change is a global effect whereas a change of water vapour concentration to the extent postulated above will be achieved, if at all, only very locally.

In any case, these radiation calculations illustrate the potentially strong impact of water vapour and even more of cirrus clouds on radiative heating rates in the upper troposphere.

### **CONTRAILS OBSERVED ON OCTOBER 18, 1989**

On Oct. 18, 1989, an unusually large number of long-living contrails formed over Southern Germany due to exceptional meteorological conditions. This was the second day in a period when from Oct. 17 till Oct. 28 a blocking high was persistent over central Europe with dominant flow at 500 hPa from southwest. The radiosonde observation of Munich of this day at noon-time, see Fig. 4, shows that the temperature decreases down to about 223 K or - 50 °C at the tropopause which occurs at an altitude of about 12 km (200 hPa in pressure level) at this time. The dew-point-temperature (dashed curve) is considerably below the actual temperature up to about 8 km, indicating dry air in the lower troposphere. In the range above 8 km, the dew-point temperature differs only by about 7 K from the actual temperature which means that the air is rather humid in this range. In fact, as shown in Fig. 5, the relative humidity, which is computed from the sounding data, is of the order 25 % below 8 km. Above 8 km the relative humidity with respect to saturation over water reaches 50 % while with respect to ice saturation it reaches about 80 %. It should be noted that such radiosonde measurements of the dew-point are uncertain up to about 2 K and this corresponds to more than 20 % in humidity (for air temperatures below -30°C) with respect to ice saturation. This error increases for lower temperatures. Hence, it seems well possible that the atmosphere above 8 km was saturated with respect to the ice phase but it was certainly unsaturated for water. The sounding in Fig. 4 shows, moreover, south-westerly winds with 15 to 30 knots in the upper troposphere.

As documented by a series of photos and movie-pictures taken from ground near Oberpfaffenhofen, the sky was clear in the morning of that day. As time went on, during the morning, more and more contrails appeared. The first ones showed up as rather narrow and straight lines. At about noon, the contrails had filled out a large portion of the visible sky. The individual contrails were rather long visible, typically 15 minutes or more. In some cases, the form of the observed ice clouds was deformed and it was not any longer clear whether they were individual sheets of clouds originated from contrails or just natural cirrus clouds. This situation is illustrated by the photo in Fig. 6. Similar observations were made on the day before and on the subsequent days.

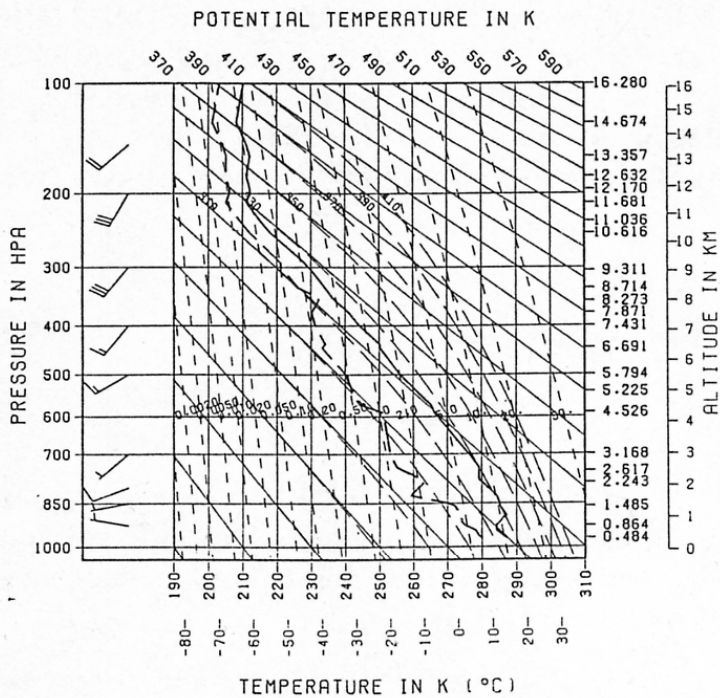


**Figure 4.** Radiosonde observation for Munich, Oct. 18, 1989, 12.00 UTC, showing wind speed and direction by wind vectors, absolute temperature (full curve) and dew-point temperature (dashed) versus altitude in a Skew-T log-P diagram.

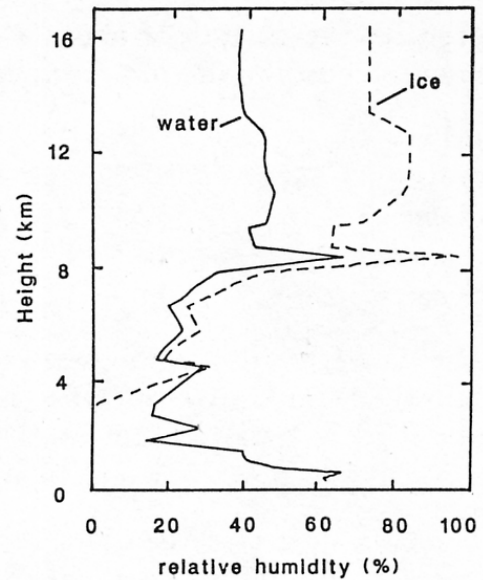


**Figure 5.** Relative humidity versus altitude relative to saturation over water and over ice.



**Figure 6.** View from Oberpfaffenhofen towards south-east on Oct. 18, 1989, 12.30 UTC (Photo by H. Höller).

At the time when the photo in Fig. 6 was taken, i.e. at 12:16 UTC (13:16 MEZ), the area was passed over by the NOAA-11 satellite on a polar sun-synchronous orbit at an altitude of about 850 km. This satellite carries among others the Advanced Very High Resolution Radiometer (AVHRR) which measures radiance from the earth with geometric resolution of about 1.1 km at nadir in five spectral channels ranging from the visible to the thermal infrared:

channel 1:	0.58 - 0.68 $\mu\text{m}$
channel 2:	0.725 - 1.0 $\mu\text{m}$
channel 3:	3.55 - 3.93 $\mu\text{m}$
channel 4:	10.3 - 11.3 $\mu\text{m}$
channel 5:	11.5 - 12.5 $\mu\text{m}$

The data from this sensor were received and processed at the DFD (German Remote Sensing Data Centre) of DLR in Oberpfaffenhofen. The processing includes computation of reflectances and of brightness temperatures from raw counts of the sensor according to prelaunch and to actual calibration factors.

The data were processed and depicted in Fig. 7 so that ice clouds become clearly visible. For that purpose we make use of the fact (Lee, 1989) that the radiative emissivity of optically thin ice clouds differs strongly in the neighbouring channels 4 and 5. Thin ice clouds are more transparent with respect to infrared radiance from below the clouds near 11  $\mu\text{m}$  than near 12  $\mu\text{m}$ . Therefore, the difference of the radiation measured in channels 4 and 5 is an effective means to identify thin ice clouds. This effect is well known and earlier has been used by us to analyze cloud heights (Pollinger and Wendling, 1984) as well as various parameters of natural clouds (Kriebel et al., 1989).

For the same scene, we produced a colour figure which has been shown on the conference and which is available from the DLR together with some explanations on a poster "Contrails observed from space", printed in 1989. The colour print is based on an even more complex nonlinear combination of all five AVHRR channels which are projected in three colours such that urban areas or those with only little vegetation appear orange-red, different kinds of vegetation appear ochre to green, coniferous forests are blue-green, water surfaces are blue, snow becomes yellow to white, and clouds are shown in light blue to grey colour. However, for the present discussion, the black and white picture (actually the blue component of the colour print) is sufficient.

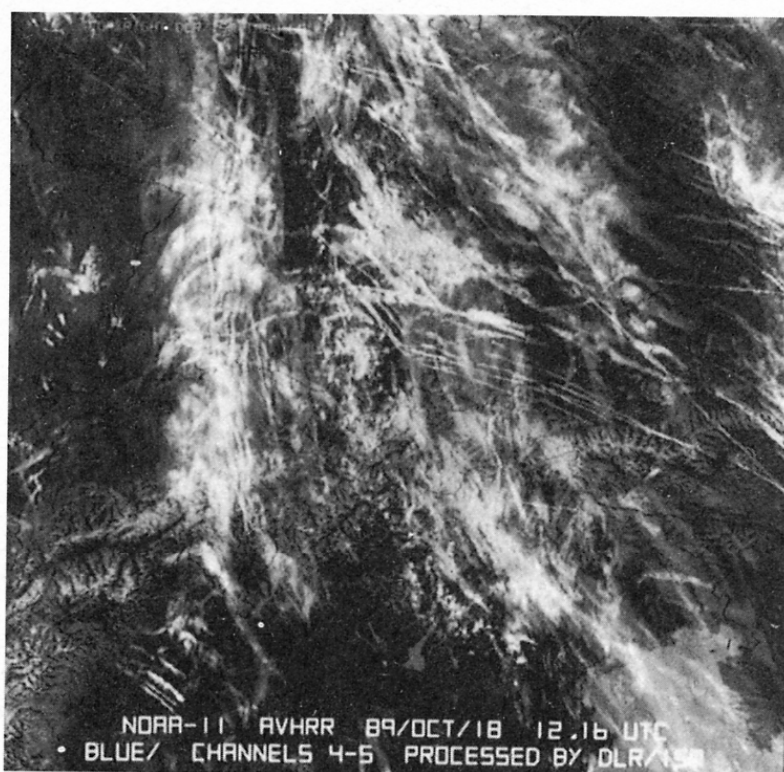


**Figure 7.**

NOAA-11-satellite on Oct. 18, 1989, 12.16 UTC in the area between Frankfurt/M. at the upper edge, Venedig and Adria at the lower edge, covering the Alps in the lower third and Kempten nearly in the centre of the picture. Note the white line-clouds which are interpreted as contrails (Processed by DLR/ISM).

Fig. 7 clearly shows that a large portion of the ice-clouds are being formed to narrow bands which very likely are contrails. The following facts support this interpretation:

- The line-forming clouds are aligned with main upper routes of air traffic as plotted in Fig. 8. This is particularly obvious for the route from Villach (VIW) in Austria over Rattenberg (RTT) passing Kempten (KPT) in the direction of the control point TGO and Frankfurt (FFM). Several other routes can be identified.
- At Kempten, this route changes its direction and this is reflected obviously by bends in the line-clouds.
- The lateral distance between individual line-clouds near Kempten is about 5 km. For a wind-speed of 20 knots (10 m/s) this corresponds to a time-difference of about 500 s or 10 minutes, which is a reasonable separation between aircrafts on upper routes.
- The visibility indicates that the clouds are either very thick or sufficiently broad to affect the measured radiance within a single pixel of about 1 km width. The observed line-clouds occasionally reach a width of several pixels, i.e. several kilometers.



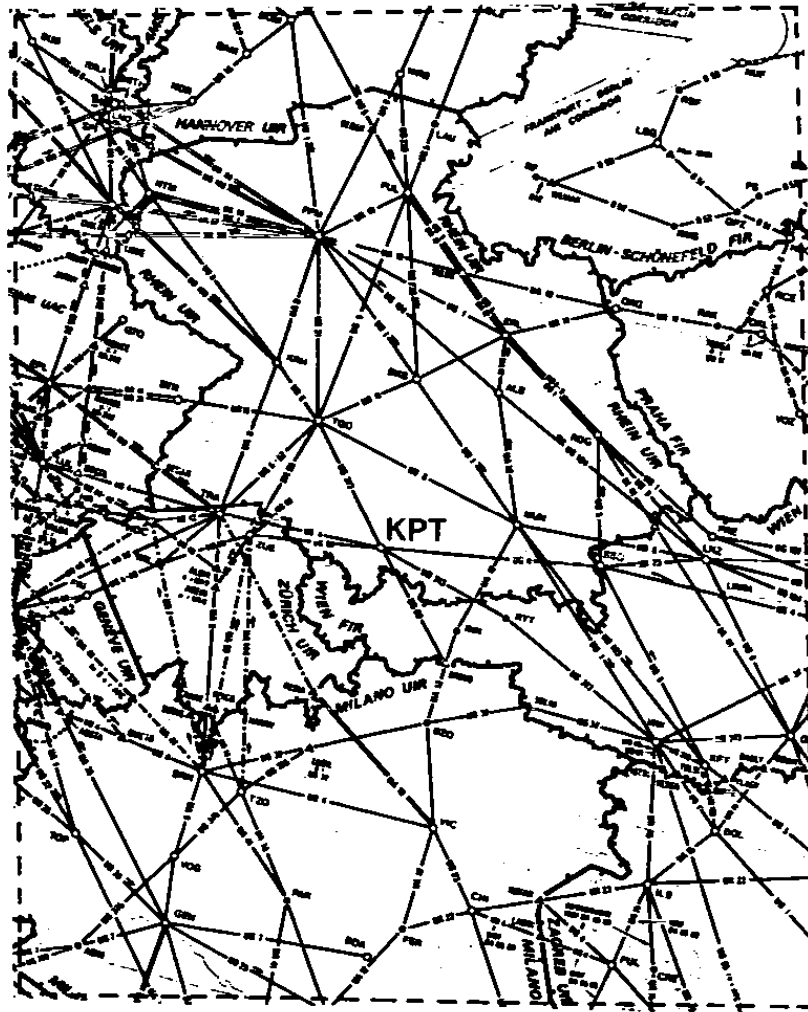


**Figure 8.** Subsection of the Air Traffic Flow Management Planning Chart, 8th ed. 1989, showing the upper traffic routes in the same area as taken by the satellite image in Fig. 7.

The last point implies that some of the rather fuzzy cirrus clouds which were observed from ground were in fact wide (up to 10 km) clouds originating from contrails.

On the other hand, the picture shows also large areas filled with rather extended and amorphous cirrus clouds. It cannot be decided whether these clouds are the remainders of old contrails or have formed naturally. Hence it is difficult to estimate the fractional area taken by contrails without any further objective criteria.

## PATTERN RECOGNITION METHOD

Obviously, an objective method is required to determine which pixel belongs to a contrail. For this purpose, a pattern recognition method has been developed. The method is similar to a method developed by Knöpfle (1988). However, Knöpfle's method does not account for different brightness values of various pixels within cloud areas.

Our method uses a mask, see Fig. 9, of 15 by 15 pixels which is carried over all pixels within the whole matrix of satellite data, i.e. the brightness temperature difference between channels 4 and 5. The centre of the mask is collocated with the pixel under investigation. Within the mask, 16 equidistant directions are distinguished which originate from the centre pixel. Along each direction the consecutive sequence of pixels forms the "mid strip". A pixel of the picture must satisfy the following three conditions before it is classified as being a pixel belonging to a contrail:

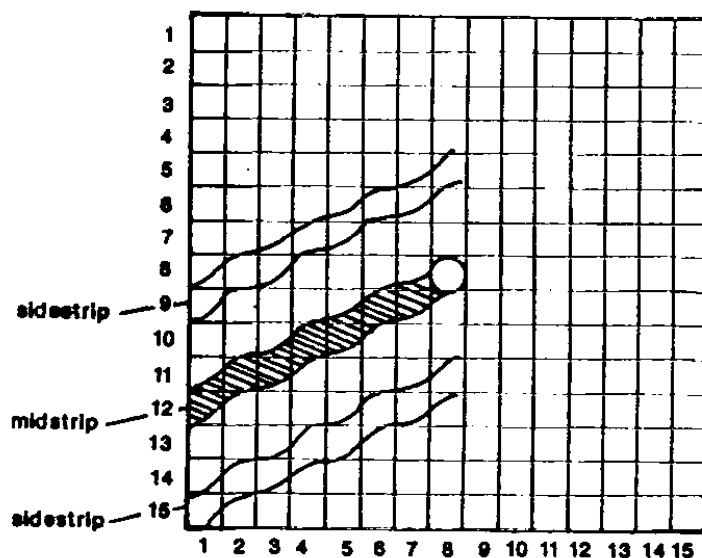


**Figure 9.** Sketch of the mask used for contrail analysis. Shown is one example of a mid-strip together with two side-strips which are used to identify contrail pixels.

- The pixel must be clouded. I.e., the temperature of the pixel must be lower than a preset threshold value.
- One of the mid-strips along the various predefined directions must be clouded. I.e., at least 5 of 7 pixels along the centre of the strip must be colder than the given limit.
- Side-strips which are parallel to the selected mid-strip but displaced by about 3 pixels sideways (see Fig. 9) must be cloud-free, i.e. their temperatures must be above a given threshold value.

The threshold values for the mid-strip and the side-strips are functions of the temperature of the centre pixel.

It happens that after one pass over the picture with this procedure some pixels are classified as being contrail pixels, which are obviously not, because they form small isolated entities without linear structure. Therefore, step 2 of the above procedure is applied a second time but now with 56 instead of 16 different radial directions.

Fig. 10 shows for example in the upper part the original data set and in the lower part the processed data set, i.e. the pixels which are classified as being contrails are identified in white. From a subjective basis, the algorithm appears to work successfully. This has been corroborated by applying the same algorithm to further data sets.

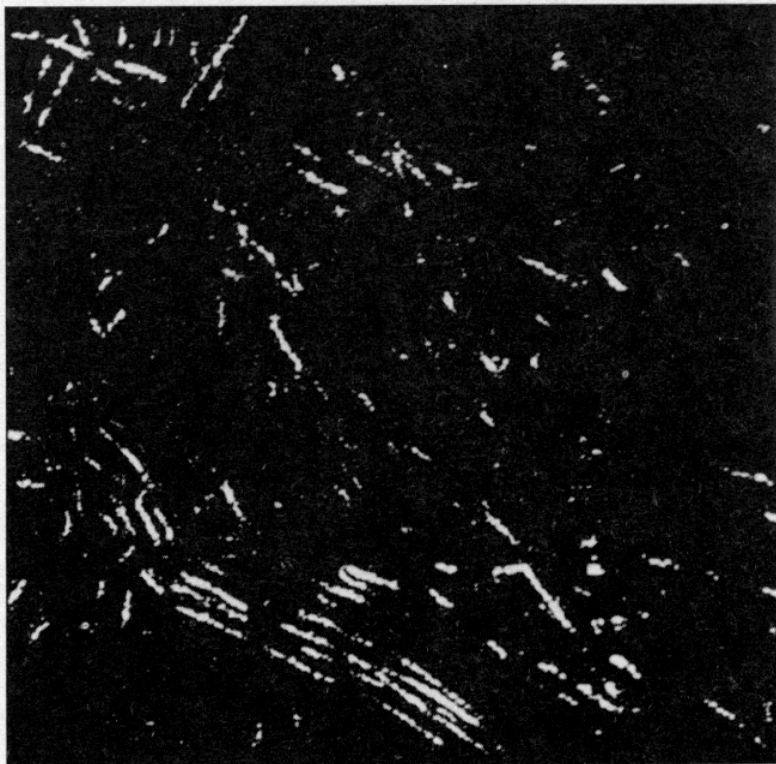
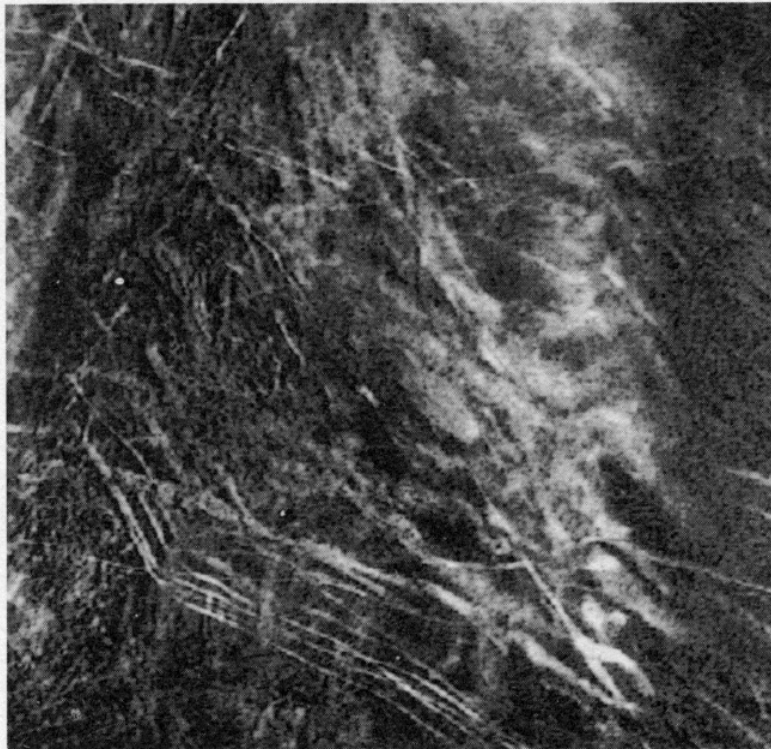


**Figure 10.** Satellite image as in Fig. 7 (top) together with the result of the contrail analysis method (white pixels in the bottom figure).

In the present case, 1 % of the pixels are classified as belonging to contrails. From a purely subjective point of view we had estimated that up to 8 % of the scene is taken by contrails. Hence, the present algorithm appears to underestimate the actual fraction taken by contrail induced clouds. This clearly shows the difficulty in deciding which pixel is cloudy or not. Improvement is expected by applying the more powerful algorithm package APOLLO (Saunders and Kriebel, 1988) to the data.

## STRUCTURE OF A CONTRAIL OBSERVED BY LIDAR

At the same time when the above observations were made from Oberpfaffenhofen, a field-experiment under the heading "International Cirrus Experiment" (ICE) took place over parts of the German Bay. The experiment included observations with a backscatter Lidar ALEX-F (Mörl et al., 1981). The laser pulses were emitted upwards from an aircraft flying at a flight level of 3700 m. The pulse length corresponds to 6 m resolution in altitude. The repetition rate allows for a resolution of about 100 m in flight direction. The measuring aircraft passed below a contrail produced by an airliner a few minutes earlier. Fig. 11 shows a composite of results including the radiosonde observation of Schleswig of that day at 12.00 UTC. The flight measurements were taken at about 13.15 UTC. From the Lidar backscatter signal one can construct contour lines of backscatter intensity. These signals can be taken as a first-order measure of ice-water content. The results in Fig. 11 show that a contrail formed at an altitude of about 8 km. The temperature at the lower edge of the contrail (7.650 km) amounts to about  $-30^{\circ}\text{C}$ . The contrail extends vertically over about 700 m and laterally over about 3.5 km. Thus the contrail became quite extended although the relative humidity with respect to ice (as deduced from the sounding) amounts to only about 50 %. It is very likely that the sounding underestimates the real humidity considerably. At altitudes between 9 and 10 km, a natural cirrus layer is observed but the measured humidity is still much below saturation. The vertical extent of the contrail is smaller than the horizontal one by about a factor of 5. This corresponds roughly to estimates of the ratio of horizontal to vertical turbulent diffusivities.

By use of the Lidar backscatter signal and a special technique the optical thickness of the contrail shown in Fig. 11 has been determined. This technique makes use of the fact that the Lidar cirrus backscatter signals show remarkable shadowing effects in presence of underlying contrails. Using this shadowing effect the Lidar system can be calibrated to determine extinction coefficients within the contrail with an accuracy of  $\pm 20\%$ . The determined optical thickness varies from about 1 at the center of the contrail to about 0.08 at the edge for a wavelength of  $1.06\text{ }\mu\text{m}$ . These data have been used to calculate the effects of such a contrail on the radiation balance at the surface. The radiative effects are calculated by using Mie theory and a two stream radiative transfer model. We assume up to now that the ice crystals consist of spheres with radii varying from  $2\text{ }\mu\text{m}$  to  $40\text{ }\mu\text{m}$ . For an averaged optical thickness of 0.2 (wavelength  $0.2\text{ }\dots\text{ }1.0\text{ }\mu\text{m}$ ) and a totally cloud covered sky our results show only a small dependence on particle size and the contrail induced cirrus cloud tend to cool the surface at noon by about  $6\text{ W/m}^2$  for a net radiation balance of the clear sky of about  $288\text{ W/m}^2$ . This means that for the considered case the contrail induced reduction in the absorbed solar radiation at ground is larger than the reduction of the outgoing longwave flux regardless of particle size.

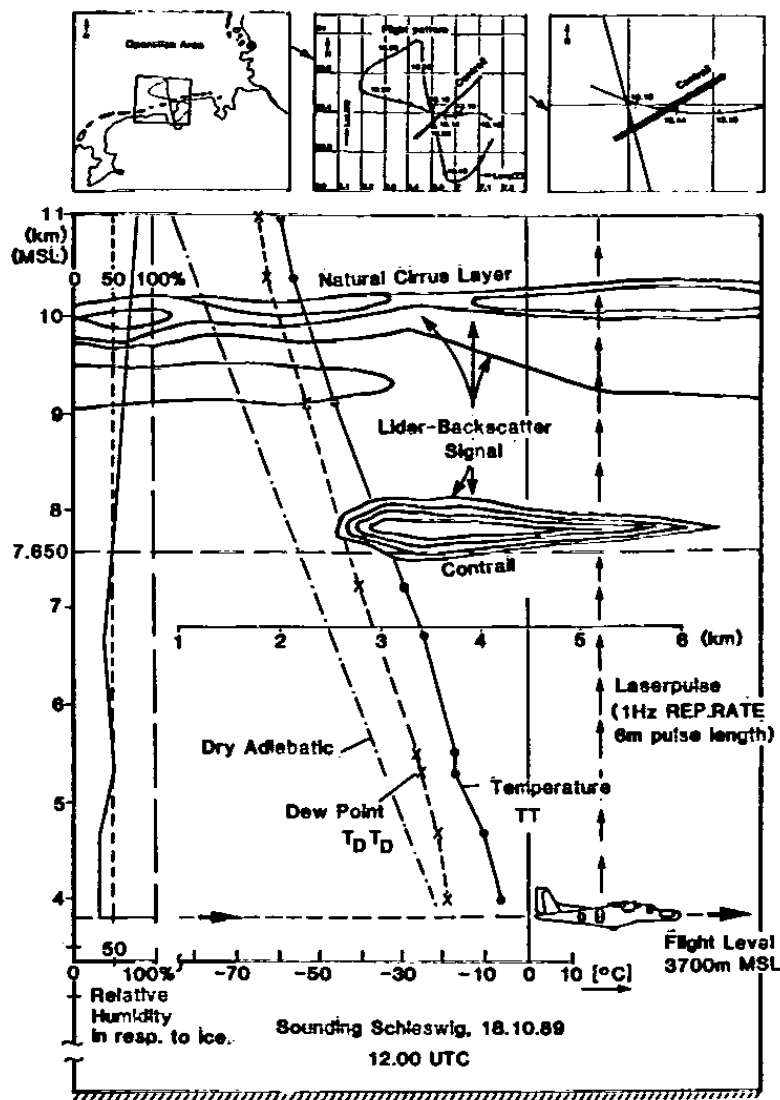


**Figure 11.** Composite picture showing properties of contrail formation over the northern shore of Germany. The upper small pictures show from left to right: the operation area, the flight pattern, and details of the flight pattern of the measuring airplane and the contrail formed by an airliner. The lower frame contains the results from the radiosonde of Schleswig and the contours of backscatter intensity of the Lidar. The lower edge of the contrail is indicated at altitude 7.650 km. The vertical and horizontal scales of the contour map are equal.

However, definite conclusions regarding the sign of the temperature change at ground cannot be made until the effects of nonspherical ice crystals are considered. Regarding to this difficult and up to now unsolved problem more research is needed in the future.

## FURTHER SATELLITE OBSERVATIONS

We have started to evaluate further satellite observations on a routine basis. Up to now, NOAA-AVHRR-data have been processed for 99 days from 8 months within a fixed area of 300000 km<sup>2</sup> between Frankfurt and Genua. At 62 days (63 % of 99) contrails were visible. For 36 of these 99 days, the area taken by contrails was below

0.1 %. For the remaining days, the average contrail coverage was estimated as 1,5 %. The present state of analysis is too preliminary to report final statistics.

Contrails are often observed in the neighbourhood of naturally occurring cirrus clouds. An example of such cases is shown in Fig. 12 from Dec. 20, 1989. Obviously, the width of contrail-induced line clouds grows considerably when approaching areas of natural cirrus clouds.

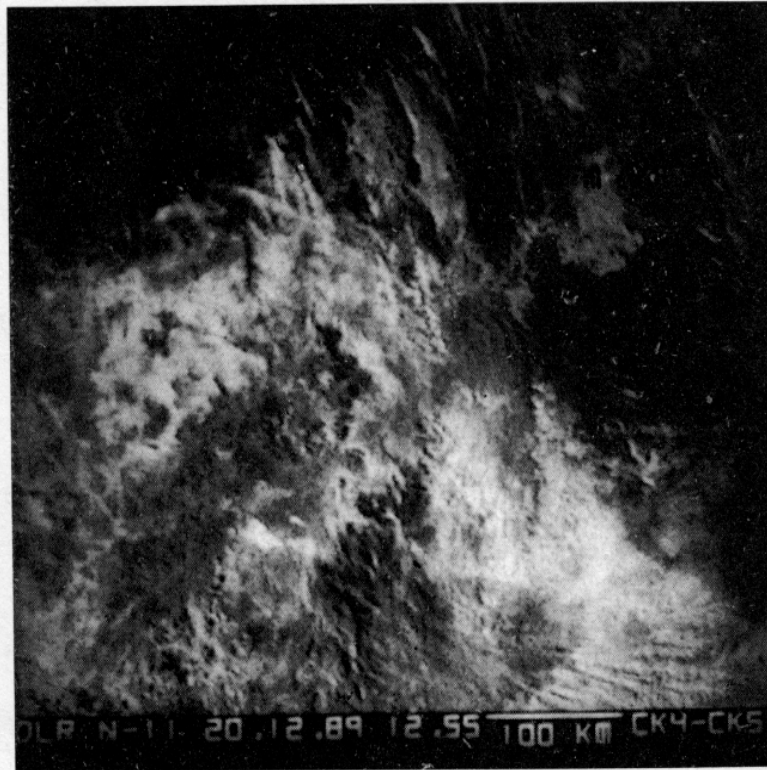


**Figure 12.** Satellite image similar to that in Fig. 7, but for Dec. 20, 1989, 12.55 UTC. The symbol "m" in the upper right corner represents the location of Munich. Note the many parallel contrails towards north-west at the northern edge of the extended cirrus cloud over the Alps in the middle of the picture.

## CONCLUSIONS

Cirrus clouds generated from contrails have the potential to strongly affect radiative heating rates in the atmosphere. The infrared heating or cooling rate magnitude within such cirrus clouds is typically a factor of two larger than that induced by water vapour increase from standard atmosphere to saturation in a 5 km thick layer near the tropopause. There are no reasons to believe that such a change can arise in a realistic manner. In fact, water vapour emissions from air traffic will cause saturation with respect to water only very locally. Nevertheless, in view of the relatively small changes induced by doubling  $CO_2$  the large radiation effects of water vapour and ice clouds are obvious. It still remains to quantify the area and volume fraction in which large increases of water vapour or contrails are caused by airliners.



Contrails may be identified from satellite data of the AVHRR in spite of its rather coarse geometric resolution (about 1 km) by computing the difference of two channels in the thermal infrared. By means of a new pattern recognition method we have a tool to deduce the contrail content of a scene on an objective basis in a repeatable manner so that one can analyse trends and regional distribution. However, this algorithm has yet been applied to a few cases only. By means of Lidar measurements, the spatial dimension of a specific contrail and its optical thickness produced by an airliner have been documented. Although the radiosondes indicate undersaturation with respect to ice and water the contrail takes considerable dimensions.

We have shown that contrails induced by air traffic on upper routes at individual days may cover a considerable portion of the sky. For the specific day of Oct. 18, 1989, which was an extraordinary case, the estimates vary from 1 to 8 % depending on the method used. A climatology is needed to estimate mean cloud covers by contrails within a longer period. Moreover, one still has to perform analysis with radiative transfer and climate models to estimate the effect of such additional (fractional) cloud cover and possible increases in water vapour concentration on the earth's climate. In view of the growing air traffic, such effects will grow with time and may become of significant importance with respect to future climate.

**Acknowledgement.** This paper is a slightly extended version of that presented by U. Schumann et al. (1990). We thank G. Gesell of the Applied Data Systems Division of the DLR and H. Höller, K.-T. Kriebel, R. Meerkötter, P. Mörl, M. E. Reinhardt, W. Renger, G. Ruppertsberg, K.-P. Schickel, and B. Strauß of the Institute of Atmospheric Physics of the DLR for their contributions and help.

## REFERENCES

- Angell, J. K., 1990: Variation in United States cloudiness and sunshine duration between 1950 and the drought year of 1988. *J. Clim.* 3, 296-308.
- Appleman, H., 1953: The formation of exhaust condensation trails by jet aircraft. *Bull. Amer. Meteorol. Soc.*, 34, 14-20.
- Beckwith, W., B., 1972: Future patterns of aircraft operations and fuel burnouts with remarks on contrail formation over the United States. *Int. Conf. Aerospace and Aeronautical Meteorol.*, May 22-26, Washington, D.C., Amer. Meteorol. Soc., Boston, 422-426. pp. 452.
- Carleton, A. M. and Lamb, P. J., 1986: Jet contrails and cirrus clouds: a feasibility study employing high-resolution satellite imagery. *Bull. Amer. Met. Soc.*, 67, 301
- Changnon, S. A., 1981: Midwestern cloud, sunshine and temperature trends since 1901: possible evidence of jet contrail effects. *J. Appl. Meteor.*, 20, 496-508.
- Held, M., 1988: Oekologische Folgen des Flugverkehrs. *Tutzing Materialien*, Ev. Akad. Tutzing, Postfach 227, 8132 Tutzing, ISSN 0930-7850, pp. 131.
- Joseph, J. H., Levin, Z., Mekler, Y., Ohring, G., Otterman, J., 1975: Study of contrails observed from ERTS 1 satellite imagery. *J. Geophys. Res.*, 80, 366
- Knöpfle, W., 1988: Rechnergestützte Detektion linearer Strukturen in digitalen Satellitenbildern. *Z. Photogrammetrie und Fernerkundung*, 56, 40-47.
- Knollenberg, R. G., 1972: Measurements of the growth of the ice budget in a persisting contrail. *J. Atmos. Sci.*, 29, 1367-1374.

- Kriebel, K. T., Saunders, R. W., and Gesell, G., 1989: Optical properties of clouds derived from fully cloudy AVHRR pixels. *Beitr. Phys. Atmosph.* 62, 165-171.
- Lee, T. F., 1989: Jet contrail identification using the AVHRR infrared split window. *J. Appl. Meteorol.*, 28, 993-995.
- Liou, K.-N., 1986: Influence of cirrus clouds on weather and climate processes: A global perspective. *Mon. Wea. Rev.*, 114, 1167-1199.
- Mörl, P., Reinhardt, M. E., Renger, E., and Schellhase, R., 1981: The use of the airborne LIDAR system "ALEX F 1" for aerosol tracing in the lower troposphere. *Beitr. Phys. Atmosph.*, 54, 403-410.
- Pfeiffer, M., Fischer, M. (Hrsg.), 1989: Unheil über unseren Köpfen? Flugverkehr auf dem Prüfstand von Ökologie und Sozialverträglichkeit. Quell Verlag, Stuttgart, pp. 239.
- Pollinger, W., and Wendling, P., 1984: A bispectral method for the height determination of optically thin ice clouds. *Beitr. Phys. Atmosph.*, 57, 269-289.
- Rotter, M., 1987: Auswirkung von Flugzeugkondensstreifen auf die Sonnenbeobachtung und auf die Bewölkungsverhältnisse in Kärnten, Dissertation, Universität Graz.
- Saunders, R. W., and Kriebel, K. T., 1988: An improved method for detecting clear sky and cloudy radiances from AVHRR data. *Int. J. Remote Sensing*, 9, 123-150.
- Schumann, U., Gesell, G., Höller, H., Kriebel, K.-T., Meerkötter, R., Mörl, P., Reinhardt, M. E., Renger, W., Schickel, K.-P., Strauß, B. and Wendling, P., 1990: Analysis of air traffic contrails from satellite data - a case study. European Propulsion Forum: Future Civil Engines and the Protection of the Atmosphere, Cologne-Porz, April 3-5, 1990. DGLR-Bericht 90-01, pp. 49-57.
- Stephens, G. L., 1989: Cirrus clouds and climate feedback: Is the sky falling and should we go tell the king? FIRE Science Meeting, Monterey, Calif., July 10-14 (sponsored by NASA et al.), p. 327- 331.
- Stephens, G. L., and Webster, P. J., 1981: Clouds and climate: Sensitivity of simple systems. *J. Atmos. Sci.*, 38, 235-247.
- Weber, G.-R., 1990: Spatial and temporal variation of sunshine in the Federal Republic of Germany. *Theor. Appl. Climatol.* 41, 1-9.
- Wetherald, R. T., and Manabe, S., 1988: Cloud feedback processes in a general circulation model. *J. Atmos. Sci.*, 45, 1397-1415.